Received: 12 August 2019 | Revised: 21 May 2020 | Accepted: 16 June 2020 | Published on: 12 July 2020

DOI: 10.1002/joc.6715

RESEARCH ARTICLE

International Journal of Climatology RMetS

Interannual to millennial-scale variability of River Ammer floods and its relationship with solar forcing

N. Rimbu[1] | **G. Lohmann**[1] | **M. Ionita**[1] | **M. Czymzik**[2] | **A. Brauer**[3]

[1]Paleoclimate Dynamics, Alfred Wegener Institute Helmholtz Center for Polar and Marine Research, Bremerhaven, Germany

[2]Marine Geology, Leibniz Institute for Baltic Sea Research Warnemünde—IOW, Rostock, Germany

[3]Climate Dynamics and Landscape Evolution, Helmholtz Centre Potsdam, GFZ German Research Centre for Geosciences, Potsdam, Germany

Correspondence
N. Rimbu, Alfred Wegener Institute Helmholtz Centre for Polar and Marine Research, Bussestrasse 24, D-27570 Bremerhaven, Germany.
Email: norel.rimbu@awi.de

Abstract

The relationship between River Ammer flood frequency variability, extreme summer climate over Europe, and solar forcing is investigated. First, we used observational data to evaluate extreme weather and climate anomaly patterns associated with flood and solar forcing as well as the possible dynamical mechanisms behind them. Then, the annual resolution flood layer record from the Lake Ammer sediments is analysed to evaluate millennial-scale variability of floods and possible related extreme climate patterns back to 5,500 years BP. A composite analysis reveals that observed River Ammer flood frequency variability at interannual to multidecadal time scales is connected to large-scale extreme precipitation and temperature patterns. From a synoptic-scale perspective, the extreme precipitation pattern associated with floods is related to an increase in the frequency of high upper-level potential vorticity (PV) events over western Europe and a decrease over eastern Europe and western Russia. Increased (decreased) frequency of upper-level high PV events is related to more (less) surface extreme precipitation occurrence. Furthermore, we show that increased frequency of upper-level high PV events over western Europe is associated with enhanced blocking activity over eastern Europe. Therefore, the out of phase interannual to millennial-scale variations of River Ammer flood frequency and solar irradiance, as presented in previous studies, can be explained by a solar modulation of eastern European-western Russia summer blocking and associated upstream upper-level wave breaking activity. In addition, we identify two distinct quasi-periodic signals in both frequency of Lake Ammer flood layer and solar irradiance records with periods of ~900 years and ~2,300 years. We argue that similar cycles should dominate millennial-scale variations of blocking activity in eastern Europe-western Russia as well as extreme precipitation and flood frequency variability over central and western Europe during the last ~5,500 years.

KEYWORDS

floods, extreme precipitation, potential vorticity, solar forcing

1 | INTRODUCTION

Over the past decades, Europe has experienced heavy floods with major socioeconomic consequences. One of these cases is the summer 2013 flood in Central Europe (Ionita *et al*., 2015), emphasizing the need for improved forecast methods of extreme hydrologic events and a better understanding of the underlying climatic processes. In particular, understanding past changes of floods on short and long timescales is crucial for anticipating the evolution of these events in response to climate change.

A focus of current climate research is on mean temperature fluctuations and less on regional changes in extreme climate events, particularly on extreme floods. Understanding the physical mechanisms behind flood variability is important for anticipating extreme climate anomalies at different spatial and temporal scales. Observational data permit the investigation of flood variability at short timescales. To study extreme precipitation and flood variability at longer timescales proxy records for extreme precipitation and floods should be used. By employing historical documents and natural archives, we can extend our knowledge back through the Holocene period or beyond. Integrating instrumental and proxy records can provide valuable information about long-term flood trends, at very high precision (Wilhelm *et al*., 2018).

The drivers of European floods are, usually, associated with specific atmospheric circulation patterns like zonal westerly or meandering regimes or VB cyclone tracks (e.g., Swierczynski *et al*., 2012). However, such circulation regimes are related not only to local extreme precipitation and floods, but could also be associated with extreme weather phenomena in more distant regions. Here, we combine instrumental River Ammer discharge data back to 1926 with the seasonally resolved flood layer time series from varved sediments of the downstream Lake Ammer covering the last 5,500 years, as well as meteorological data to investigate the mechanisms behind interannual to millennial flood variability. Detecting such features can improve the interpretation of the flood layer record from Lake Ammer sediments (Czymzik *et al*., 2010), in terms of extreme weather and climate variations. The main goal of this paper is to relate River Ammer flood frequency variability from the discharge and lake sediment records with extreme climate anomaly patterns as well as to identify the dominant forcing of flood variability on up to millennial timescales.

Previous studies have shown that extreme precipitation phenomena are associated with upper-level atmospheric circulation patterns (e.g., Schlemmer *et al*., 2010; Barton *et al*., 2016). Due to conservation of potential vorticity (PV), significant features that are related to synoptic-scale weather systems, responsible for extreme precipitation, can be identified and followed in space and in time. River Ammer floods are related to specific upper-level PV patterns (Rimbu *et al*., 2016). Here we investigate the possible role of solar forcing on River Ammer flood frequency variability through such upper-level PV patterns.

This article is organized as follows. Data and methods are presented in Section 2. The results are presented in Section 3. The relationship between observed daily River Ammer floods with extreme climate and upper-level atmospheric circulation is discussed in Section 3.1. In Section 3.2, the possible role of atmospheric blocking on the observed solar forcing-flood relationship is discussed. Section 3.3 discusses the millennial-scale variability of flood layer frequencies in the Lake Ammer sediments and its possible implications for extreme climate variability throughout the last 5,500 years. A summary and the main conclusions are given in Section 4.

2 | DATA AND METHODS

The main quantity analysed here is daily mean River Ammer runoff recorded at Gauge Weilheim (Bayerisches Landesamt für Umwelt, 2007) covering the period 1926 to 2015. River Ammer rises in the Bavarian Alps and flows northward for about 80 km to Lake Ammer (48.01°N; 11.12°E). Details about River Ammer and its catchment can be found in Ludwig *et al*. (2013) and Petrow and Merz (2009). Here we examine the observed daily discharge of River Ammer during summer (June, July, August), the main flood season in the River Ammer region (Czymzik *et al*., 2010, 2013). We combine the measured discharge data with the 5,500-year flood layer record from varved Lake Ammer sediments, a proxy for River Ammer flood frequency in spring and summer (Czymzik *et al*., 2010). A daily River Ammer discharge, greater than 125m^3/s is associated with a flood, since above this threshold the deposition of a flood layer in the investigated lake Ammer sediments is very likely (Czymzik *et al*., 2010). Millennial-scale variability in the lake sediment record, a proxy for River Ammer floods during the last 5,500 years (Czymzik *et al*., 2016) is analysed in connection with solar forcing. The flood layer time series is available at the environmental database PANGAEA (https://doi.pangaea.de/10.1594/PANGAEA.803368).

The R20mm index describes the number of days in summer with total daily precipitation higher than 20 mm (e.g., Zhang *et al*., 2011). It is analysed in connection with observed River Ammer flood variability. As a measure of extreme temperature we have used the summer day (SU)

index, defined as the number of days in summer with a maximum daily temperature (TX) above 25°C. These indices are calculated based on daily precipitation and maximum daily temperatures from the E-OBS data set (e.g., Cornes *et al*., 2018).

Previous studies (Browning, 1997; Schlemmer *et al*., 2010) have emphasized a strong relationship between upper-level potential vorticity (PV) anomalies and precipitation extremes. Southern intrusions of air with relatively high PV in the upper troposphere or lower stratosphere are commonly accompanied by a local lowering of the dynamic tropopause, intense vertical motions, high vertically integrated water vapour transport, rapid cyclogenesis, intense convection and heavy rainfall (e.g., Krichak *et al*., 2014). The height of the dynamic tropopause is commonly defined as the level at which PV equals 2.0 PV units (PVU). In the troposphere, PV is ordinarily below this value and relatively uniform, but in the stratosphere, it is much higher due to increased stability. PV gradients are large in polar regions, where a particular isentropic surface lies in the stratosphere, but are weak further southward. Usually, the 2 PVU contour on an isentropic surface that lies in the stratosphere in the polar region is noticeably contorted showing long tongues of high PV air extended outward. Such PV streamers are associated with extreme mid-latitude weather (e.g., Schlemmer *et al*., 2010). Cut-off lows, which appears as small regions of high PV air totally encircled by low PV air, are also related to extreme surface precipitation and floods. Here, we investigate the relationship between River Ammer floods and PV patterns on the 330 K isentropic surface. We look also at the relationship between the frequency of high upper-level PV days, that is, PV on 330 K surface greater than 2.0 PVU, and solar irradiance forcing. The PV patterns remain qualitatively the same if the analysis is performed on isentropic surfaces varying from 320 K to 340 K. PV on the 330 K isentropic surface is calculated using temperature and horizontal wind field from NCEP1 reanalysis (Kalnay *et al*., 1996) for 1948 to 2015 summers. The same quantity, i.e. PV on the 330 K surface, covering the 1836–2015 period, was extracted from the 20CR V3 data set (Slivinski *et al*., 2019) and used to derive flood and solar-related PV patterns at interannual to multidecadal timescales.

Daily 500 hPa geopotential height (Z500) data from the NCEP1 reanalysis (Kalnay *et al*., 1996) is used to construct blocking frequency for the period 1950–2015. We calculate the two-dimensional blocking index as described by Scherer *et al*. (2006), which is an extension of the classical one-dimensional blocking index of Tibaldi and Molteni (1990). As the horizontal resolution of Z500 field is 2.5° longitude × 2.5° latitude, a latitudinal gradient of 15° north and south is taken around each grid point from 35°N to 75°N to calculate the Z500 gradients. A grid point is considered as blocked if the northern Z500 gradient is less than −10 m/(deg. latitude) and the southern Z500 gradient is positive. The time persistence threshold, considered here, is one day. Therefore, this index captures blocking like circulations or instantaneous blocking, as it is often referred to in the literature (e.g., Davini *et al*., 2012). The blocking pattern associated with low solar forcing is calculated as the average blocking frequency anomaly maps for all summers characterized by a solar activity index smaller than minus one standard deviation.

Two solar activity reconstructions are used in this study. The first is the open solar flux (Lockwood *et al*., 2009) derived from geomagnetic measurements. It exhibits stronger correlations with atmospheric circulation variations than conventionally used measures of solar activity (Woolings *et al*., 2010). Open solar flux data at annual resolution are available at the KNMI webpage (www.knmi.nl). Based on this record, we construct the blocking frequency as well as upper PV patterns associated with low solar activity during the observational period. The second is the Holocene total solar irradiance (TSI) reconstruction of Steinhilber *et al*. (2009), which is used to analyse the relationship between millennial-scale TSI variability and frequency of flood layer in the Lake Ammer sediments during the last ~5,500 years (Czymzik *et al*., 2016). Singular spectrum analysis (SSA) (e.g., Ghil *et al*., 2002) was applied to search for quasiperiodic signals in the TSI and flood layer records.

3 | RESULTS

3.1 | Extreme climate patterns associated with River Ammer floods during the observational period

Based on daily River Ammer discharge we identify flood years, that is, years with at least one day of River Ammer discharge above 125m^3/s. The frequency of flood years (Figure 1) is relatively high from 1950 to 1981 and 2000 to 2015. No flood days are recorded during summers from 1982 to 1999 (Figure 1). Interestingly, during this period solar activity was relatively high. 8(5) out of 13 flood years occur during summers with a solar irradiance activity below the mean (minus one standard deviation). Note also that the River Ammer flood in summer 2010, when enhanced blocking activity was recorded in the Eastern Europe (Drouard and Woolings, 2018), is associated with very low solar irradiance (Figure 1).

River Ammer floods are related to heavy rain in the catchment area during spring and summer (e.g., Czymzik *et al*., 2010). We address the question of the spatial

extension of the extreme precipitation anomalies causing River Ammer floods during summer. The composite map of the R20mm index shows that River Ammer floods are associated with more frequent extreme rainfalls over parts of central, western, and southern Europe (Figure 2a). The pattern is consistent with enhanced precipitation in the Ammer region 1 day before the onset of each daily River Ammer flood from 1950 to 2015 period (Figure S1). Similar patterns are obtained for other extreme precipitation indices, like R10mm, Rx5day and R95PTOT (not shown). The composite map of the SU index (Figure 2b) shows a decrease (increase) in the frequency of summer days over western, central, and southern Europe (southwestern Europe, northeastern Europe and western Russia) during flood years relative to the climatology. Both patterns are consistent with the precipitation and temperature anomaly patterns associated with observed River Ammer floods (Rimbu *et al.*, 2016). We conclude that River Ammer floods are associated with large scale extreme precipitation and temperature patterns.

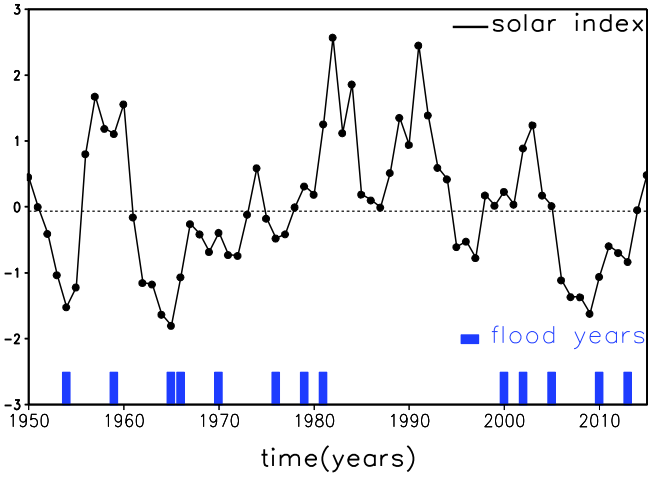

FIGURE 1 River Ammer summer flood years (vertical bars) and solar activity index (solid line) for 1950–2015 (see text for details)

To understand how floods are related to extreme temperature and precipitation (Figure 2) we look first at atmospheric circulation patterns associated with daily River Ammer floods, that is, daily discharge higher than 125 m^3/s. Correlation analysis reveals that River Ammer daily discharge and local daily precipitation are maximally correlated at one-day time lag (not shown). Therefore, we look at the upper level PV maps, 1 day before the onset of a daily River Ammer flood. Most of the observed daily floods from the 1950 to 2015 period are associated with high PV values (PV > 2PVU) in the Ammer region (Figure S2). The PV patterns have various spatial structures, including streamers, cutoffs, or troughs. For most of the flood events relatively low PV values are recorded over southwestern Europe and eastern Europe-western Russia (Figure S2).

The composite map for upper-level circulation during all River Ammer flood days (Figure 3a) shows a pronounced trough over western Europe, consistent with previous studies (Rimbu *et al.*, 2016). However, this

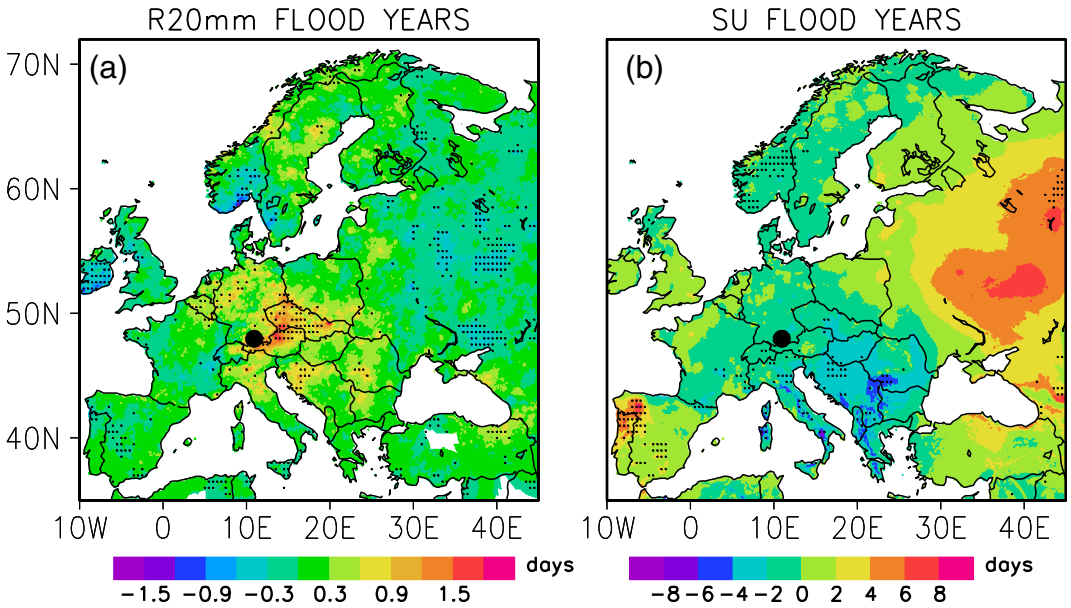

FIGURE 2 Composite maps of (a) R20mm index (summer days with very heavy rainfall) and (b) SU index (summer days with extremely high temperatures) for flood years during 1950–2015. Filled black circles depict the location of the Ammer region. Hatching display areas at or over the 90% significance level. Units: Days

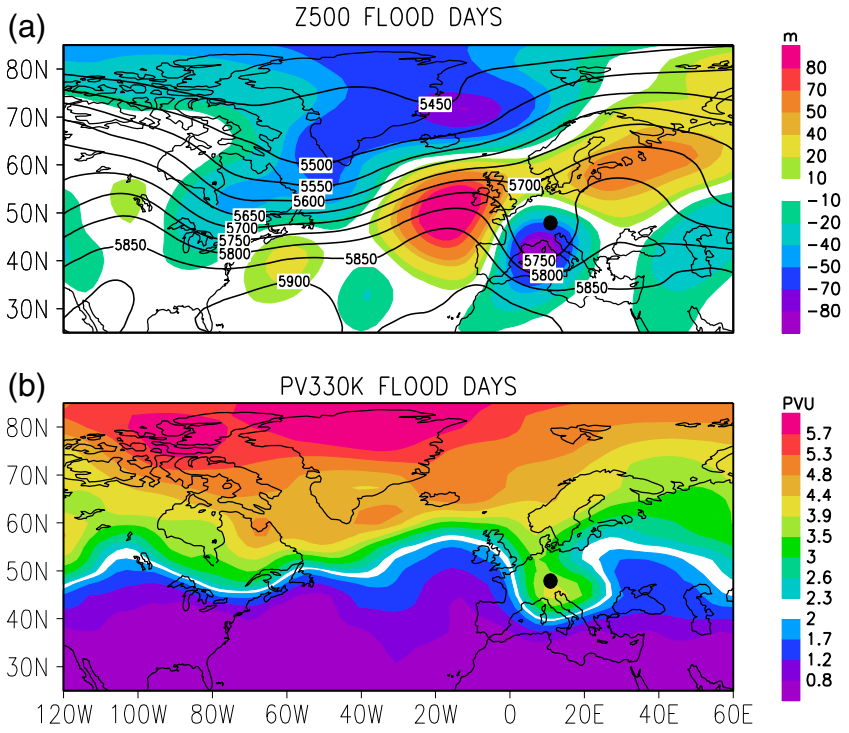

FIGURE 3 Composite map of daily (a) Z500 (contour) and Z500 anomalies (shaded) and (b) potential vorticity on 330 K potential temperature surface for observed daily River Ammer floods during summers from 1950 to 2015. Filled black circles depict the location of the Ammer region. Units: m and potential vorticity units (PVU)

trough is part of a large-scale wave pattern that extends downstream over the Atlantic. The wave-structure is clearly emphasized on the PV distribution on the 330 K potential temperature surface (Figure 3b). This wave, which shows an increasing amplitude over the North Atlantic, breaks over western Europe. The relatively high (low) PV values prevail over the region with an increased (decreased) frequency of extreme precipitation (Figure 2a), consistent with the strong connection between upper-level PV anomalies and surface extreme precipitation (Schlemmer *et al.*, 2010; Krichak *et al.*, 2014). A similar analysis of 20CRV3 PV data, going back to 1926, reveals that daily River Ammer floods are associated with a hemispheric scale pattern with wave-number ~6 (Figure S3). Similar patterns were related to the dramatic increase in recent Northern Hemisphere summer extreme temperature and precipitations through the quasi-stationary resonance (QRA) mechanism (Petoukhov *et al.*, 2013; Kornhuber *et al.*, 2016).

3.2 | The role of atmospheric blocking

Atmospheric blocking plays a central role in generating extreme precipitation and temperature anomalies (e.g., Woolings *et al.*, 2018). Here we investigate the relationship between summer blocking, River Ammer floods, and solar forcing during the 1950–2015 summers.

The 2D instantaneous blocking frequency climatology for the Atlantic-European region is displayed in Figure 4.

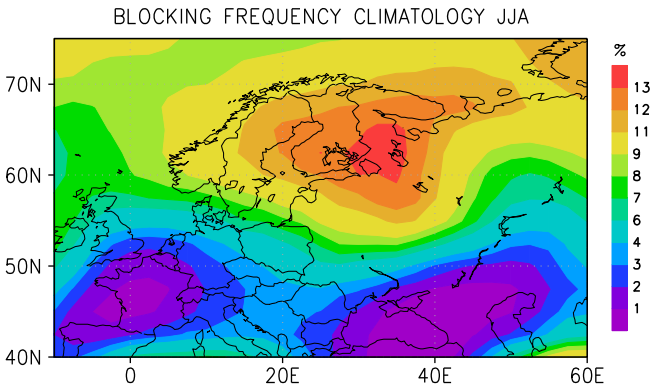

FIGURE 4 Summer blocking frequency climatology. The period is 1950–2015. Units: percent of blocked days from total number of summer days

It shows a relatively high blocking frequency (9–13% of all days) over the Scandinavian region. Another high-frequency centre (9–11% of all days) is recorded over northwestern Russia, near Novaya Zemlya. The position of the high blocking frequency band is connected with the position of the jet stream during summer (Masato *et al.*, 2013). Previous studies of two-dimensional summer blocking frequency (Masato *et al.*, 2013; Woolings *et al.*, 2018) reveal similar blocking patterns over this region.

The composite map of blocking frequency anomalies for observed summer River Ammer floods (Figure 5a)

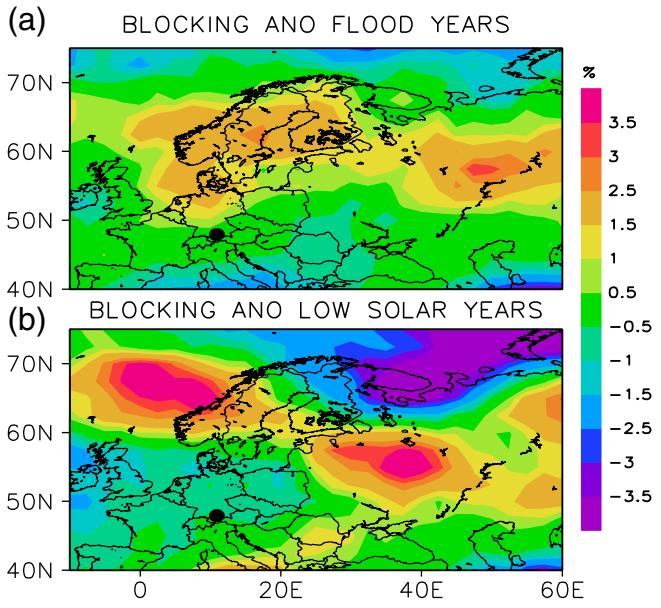

FIGURE 5 Blocking frequency anomaly for (a) observed River Ammer flood years and (b) low solar irradiance years. The period is 1950–2015. Filled black circles depict the location of the Ammer region. Units: percent of blocked days from total number of summer days

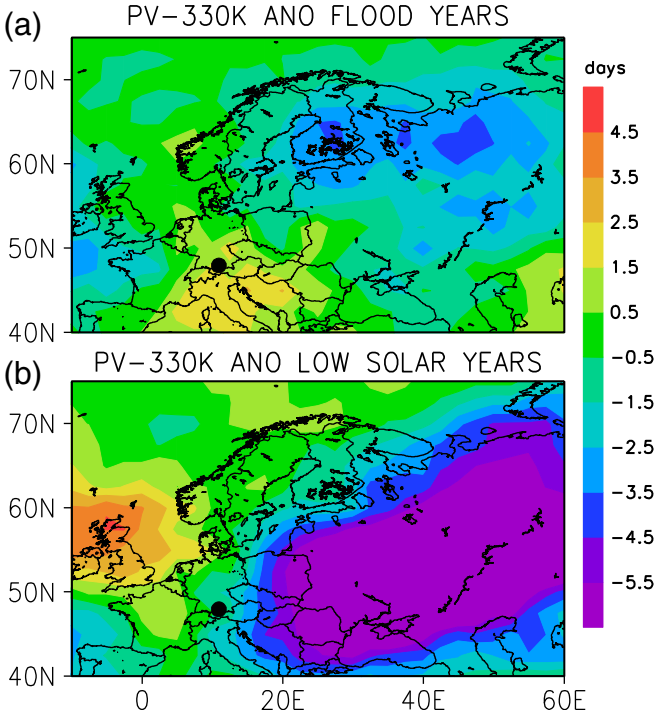

FIGURE 6 Anomaly in the frequency of high PV days (PV on 330 K surface higher than 2.0 PVU) for (a) flood years and (b) low solar irradiance years from 1950 to 2015. Filled black circles depict the location of the Ammer region. Units: days

depicts positive anomalies over northern and northeastern Europe. In these regions, positive Z500 anomalies are recorded during daily floods (Figure 3a). Interestingly, a similar blocking pattern is associated with low solar irradiance summers during the same period (Figure 5b). This is consistent with an increased flood frequency during low solar irradiance summers as shown in Figure 1.

The PV composite map associated with observed daily River Ammer floods (Figure 3b) suggests a possible upper-level atmospheric forcing on flood variability. We consider the number of days in a summer with high upper level (i.e., 330 K surface) PV values (PV > 2PVU) as a measure of upper-level atmospheric forcing on extreme surface precipitation and floods. Positive anomalies of this index can be linked to more frequent upper-level high PV structures, like streamers or cutoffs. Such PV patterns increase the probability of extreme surface precipitation and floods (e.g., Krichak *et al.*, 2014). Consistent with the PV structures during individual daily floods (Figure S2), more (less) frequent high PV days at upper levels are recorded over western Europe (eastern Europe and western Russia) during River Ammer flood summers (Figure 6a). A similar pattern is associated with low solar irradiance summers (Figure 6b). Overall, there are some inconsistencies between the blocking (Figure 5) and PV (Figure 6) corresponding patterns. These can be related to the relatively short time-span covered by the NCEP1 data as well as to the characteristics of the applied blocking and PV indices.

To better assess and confirm the relationship between solar forcing and upper-level PV, as shown in Figure 6b, we used the 20CRV3 PV data (Slivinski *et al.*, 2019) to extend the analysis back to 1836. The time series of a regional index (RPV), defined as the average of PV indices described above in all grid points within the (30–60°E; 40–55°N), and solar irradiance (Figure S4a) are significant (95% level) positively correlated (r = .24). Negative values of RPV are associated with more frequent blocking days in this region. Correlations between this index and R20mm extreme precipitation indices over central and western Europe during 1950–2015 are predominantly negative (Figure S4b). On synoptic scales, a blocking over northeastern Europe favours the occurrence of wave breaking and heavy precipitation over western Europe (e.g., Barton *et al.*, 2016). We propose the same mechanism to explain the solar-flood connection described above. More frequent blocking events over eastern Europe-western Russia during low solar irradiance summers lead to more frequent wave breaking events over western Europe, a less stable vertical atmosphere, and more frequent floods.

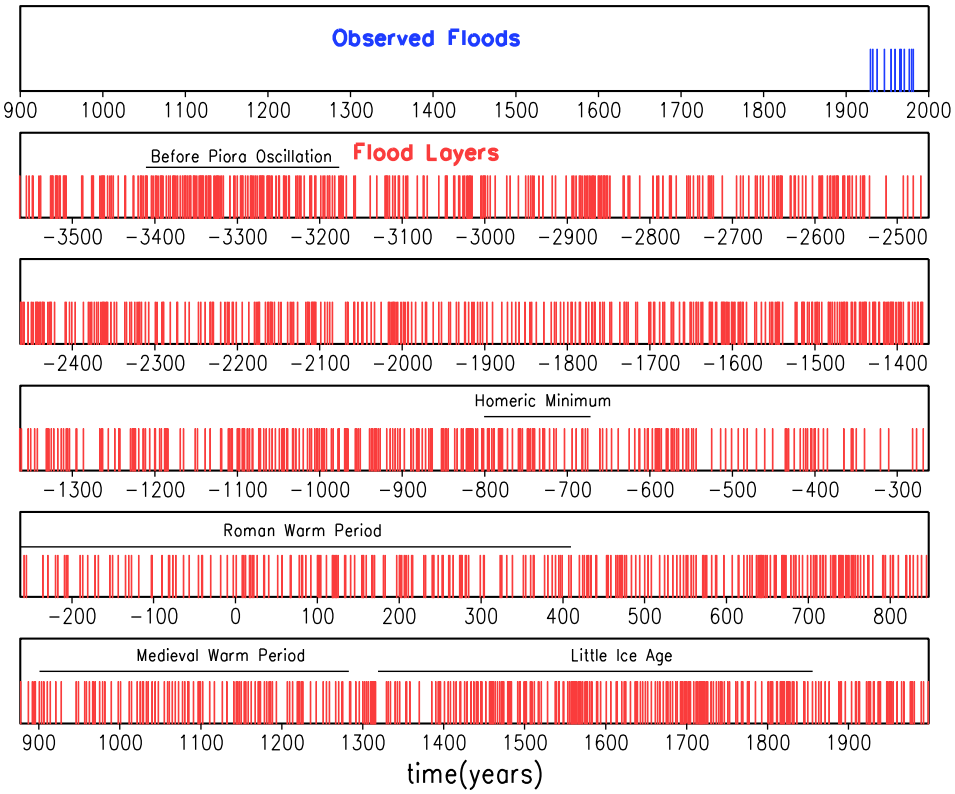

FIGURE 7 Time series of observed River Ammer flood years for the period 1926–1999 AD (blue bars) and flood layer years (red bars) for the period 3,550 BP to 1999 AD

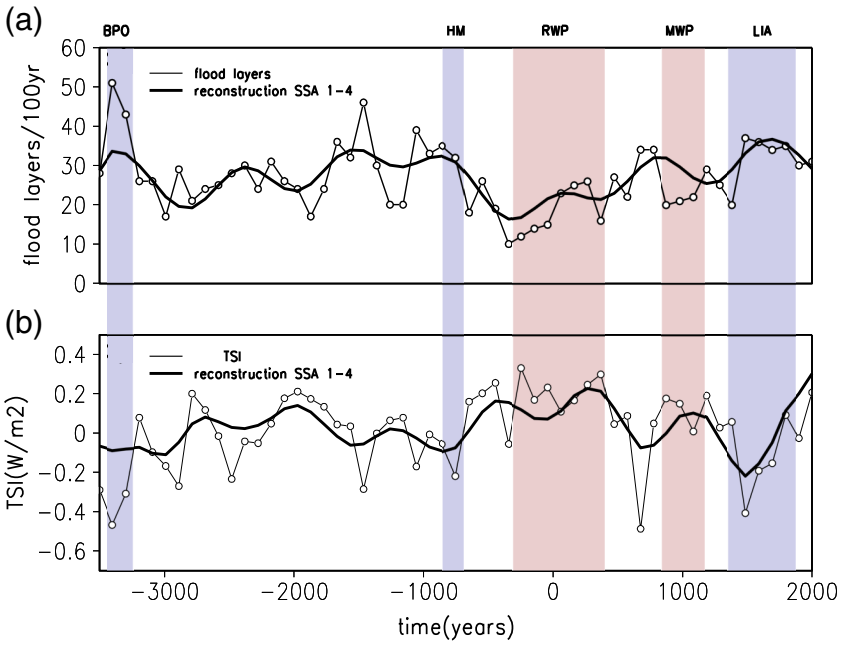

FIGURE 8 (a) Time series of the frequency of flood layer years in a 100-year window (thin) and its reconstruction from the first four SSA components (thick). (b) Time series of 100-year TSI anomaly averages (thin) and its reconstruction from the first four SSA components (thick) (see text for details)

Anomaly patterns of our PV index, i.e. the number of days with PV higher than 2PVU, linked to solar forcing resemble each other on interannual and multidecadal time scales (Figure S5). This similarity suggests that solar irradiance changes modulate extreme precipitation and flood variability over western and central Europe through the same mechanism on interannual and multidecadal timescales.

3.3 | Flood layer variability during the last millennia

The frequency of flood layers of Lake Ammer sediments shows strong interannual to millennial variability during the last 5,500 years (Figure 7). Periods with low flood frequency lasting from several decades to centuries occur often during this period. High flood frequency is recorded

during 3,400 BC–3,200 BC, immediately before the Piora Oscillation (BPO) or Piora Cold Period (Figure 7). The Piora Oscillation, named after the Piora Valley in Switzerland, was an abrupt cold and wet period in the Alpine region dated to about 3,200 BC–2900 BC (e.g., Wick and Tinner, 1997). Another period with high flood frequency is the Homeric Minimum (HM) (Figure 7). The HM is a grand solar minimum that took place between 800 BC and 600 BC (e.g., Martin-Puertas *et al*., 2012). During this period wet conditions were recorded over western Europe, while dry conditions prevailed over eastern Europe, consistent with extreme precipitation patterns associated with River Ammer floods during the observational period (Figure 2a).

More frequent flood layers occur during the Little Ice Age (LIA; ~1,300 AD–1850 AD), a period characterized by low temperatures over Europe (e.g., Kaniewski *et al*., 2016) (Figure 7). Low frequency of flood layers is recorded during warm periods like the Roman Warm Period (RWP; ~250 BC–400 AD) or Medieval Warm Period (MWP; ~900 AD–1,300 AD). The variability in the frequency of observed flood years is not unusual in the perspective of the last ~5,500 years (Figure 7).

Previous studies (e.g., Czymzik *et al*., 2016) show that River Ammer flood frequency is significantly negatively correlated with total solar irradiance (TSI) on decadal to centennial timescales. Here, we focus on millennial-scale variations of the flood layer record and its relationship with the TSI reconstruction of Steinhilber *et al*. (2009) throughout the last 5,500 years. The analysis is based on the frequency of flood layers and TSI anomalies in a non-overlapping 100-year moving window for the common period which is 3,500 BC–1999 AD. A simple visual inspection of the flood frequency and anomaly TSI time series (Figure 8) reveals that periods of high flood activity are associated with low solar irradiance. For example, relatively high flood frequency is recorded during 3,400 BC–3200 BC, when TSI was relatively low. A similar relationship is present during the LIA (Figure 8). Less flood activity is recorded during high solar irradiance periods like RWP or MWP (Figure 8).

An SSA (Ghil *et al*., 2002) isolates two distinct millennial-scale cycles in flood frequency between 3,500 BP and 1999 AD. The first cycle has a period of ~2,300 years and the second ~900 years. Together they describe ~60% of the centennial to millennial-scale flood frequency variability (Figure 8a). A similar SSA of the TSI time series identifies two cycles with similar periods (Figure 8b). The reconstructed flood and TSI signals from these two cycles during the last 5,500 years are broadly anti-phased (Figure 8). Most of the warm or cold Holocene periods are associated with maxima or minima of the signal reconstructed from these two cycles.

4 | DISCUSSION AND CONCLUSIONS

In this study, we investigated the observed and proxy River Ammer flood variability and its relationship to solar irradiance forcing during summer. It was shown that atmospheric blocking occurs with a higher probability over eastern Europe-western Russia during summers characterized by low solar activity. Increased blocking frequency in this region is associated with positive anomalies of extreme precipitation indices over central and western Europe, including the Alpine region. This explains, from a synoptic-scale perspective, the out-of-phase variations of solar irradiance and River Ammer flood frequency, as reported in previous studies (e.g., Czymzik *et al*., 2016). Recently, Drouard and Woolings (2018) investigated the processes that initiate blocking events over western, central, and eastern Europe-western Russia during summer. They showed that blocking over eastern Europe-western Russia is preceded by significant low-frequency, large-scale wave trains (their Figure 1c) that resemble the Northern Hemisphere atmospheric circulation pattern associated with River Ammer floods, presented in this paper (Figure S3). Similar patterns are related to the significant increase in extreme summer temperature and precipitation during recent decades (Petoukhov *et al*., 2013; Kornhuber *et al*., 2016). We argue that this pattern, which favours enhanced blocking activity in eastern Europe (Drouard and Woolings, 2018), could be enhanced during low solar irradiance summers. Enhanced blocking activity in this region increases the probability of upper-level wave-breaking and surface extreme precipitation over western Europe (Barton *et al*., 2016). However, the relationship between solar irradiance and other forcing on wave breaking across the western Europe, like ridges over the central Atlantic or extra-tropical transition events over the western Atlantic and North America (e.g., Barton *et al*., 2016), should also be investigated.

The influence of solar activity on weather and climate variability has received significant scientific attention for winter but less for summer. Significant modulation of solar forcing on the frequency of synoptic types winter atmospheric circulations was reported (e.g., Huth *et al*., 2008). The solar irradiance forcing can modulate the frequency of extreme precipitation and floods through modulation of the frequency of the related atmospheric circulation types. Furthermore, statistical analysis of long-term instrumental, historical, and proxy data sets reveals that large-scale teleconnection patterns are associated with decadal to multidecadal solar irradiance forcing (Lohmann *et al*., 2004). Various dynamical mechanisms have been proposed to explain the solar influence on

winter surface climate, such as the downward propagation of polar vortex anomalies (Ineson *et al*., 2011), synoptic-scale Rossby wave breaking (Lu *et al*., 2013), or eddy momentum fluxes (Simpson *et al*., 2009). Using modelling experiments, Haigh (1999) reported a weakening and broadening of the tropical Hadley cells accompanied by polewards moving of the sub-tropical jets and mid-latitude Ferrel cells during high solar irradiance years. This causes sub-tropical warming and a characteristic vertical banding of mid-latitudes temperature changes in both the summer and winter hemispheres. The enhanced summer blocking over eastern Europe during low solar irradiance summers reported here could be related to a direct impact of Sun on summer climate or could be a result of persistence of winter anomalies induced by the Sun through the subsequent summer (e.g., Ogi *et al*., 2003). Also, blocking over eastern Europe could be amplified through diabatic processes associated with weather systems that generate heavy precipitation (Pfahl *et al*., 2015). Furthermore, the possibility that solar irradiance forcing to set the conditions to increase the probability of occurrence of QRA events, a pattern responsible for summer extremes (e.g., Kornhuber *et al*., 2016) should also be investigated.

Analysing observational daily River Ammer discharge data revealed that during summer floods, extreme precipitation occurs with a higher probability over large areas of central and western Europe. Further empirical associations between flood frequency and solar activity in records from the Atlantic-European region support the larger spatial relevance of the flood signal from the River Ammer catchment (Czymzik *et al*., 2016). In our study, we describe the anomaly patterns of extreme precipitation and temperatures associated with River Ammer floods during the observational period and show that they are similar to the corresponding patterns associated with low solar irradiance. Furthermore, we argue that such patterns remain qualitatively the same for different timescales. Therefore, these patterns might be used to systematically search for a solar signature in different proxy records during the past. For example, during the period of the Spörer Minimum (SPM) in solar activity, that is, ~1,400 AD–1,510 AD, major flood events were documented in the eastern part of the Carpathian basin, Bohemia, Austria and the Hungarian Kingdom (Camenisch *et al*., 2016 and references therein). In the same period River Ammer flood frequency was relatively high (Figure 7). This supports the hypothesis that particular flood records are related to large-scale extreme precipitation patterns and solar irradiance is a possible forcing. However, extreme climate conditions, like those during the early solar Spörer Minimum (SPM) around 1,430 AD are related not only to the solar irradiance forcing but to a superposition of internal and external factors (Camenisch *et al*., 2016).

Previous studies (Czymzik *et al*., 2016) identified significant low-frequency oscillations,with periods around 90 and 210 years, in the mid to late Holocene flood layer record from Lake Ammer sediments and connected with the solar Gleisberg and Suess cycles. Their analysis reveals also a dominantly anti-phase behaviour between frequency of flood layers and TSI at these time scales (Czymzik *et al*., 2016). Here, we show that about 60% of the centennial to millennial flood layer variability is described by two cycles with periods around 900 and 2,300 years. Kaniewski *et al*. (2016) identified persistent ~900 and ~2,300 year cycles in the records of storm surges, coastal flooding, and agricultural losses from the central Mediterranean. Comparable cycles were identified in Alpine paleoflood records by Wirth *et al*. (2013) and in the dominant mode of North Atlantic Holocene temperature variability (Rimbu *et al*., 2004). We identified similar cycles in the TSI reconstruction by Steinhilber et al. (2009), usually referred to as the Eddy (~900 years) and the Hallstatt (~2,300 years) cycle respectively. They are the longest studied direct tracers of solar activity. Both cycles were also found in the Solanki *et al*. (2004) solar irradiance reconstruction through a singular spectrum analysis (Dima and Lohmann, 2009). There are furthermore speculations that both cycles are of astronomical origin (Scafetta *et al*., 2016). Our analysis reveals that the atmospheric circulation patterns associated with flood frequency variability and low solar forcing are qualitatively the same for interannual to multidecadal timescales (Figure S5). If they remain so also for centennial to millennial timescales, a hypothesis that should be confirmed through numerical model experiments, the corresponding precipitation and extreme temperature patterns associated with low solar forcing might be also independent on timescale, and, to a certain degree, be anticipated.

Our analysis reveals that flood frequency and solar variability are associated with distinct spatial and temporal patterns in blocking frequency, extreme temperature, and precipitation over Europe during summer. To date, however, the mechanistic explanation of Sun-climate connections focused on the winter season. Therefore, model experiments should be performed to assess the robustness of these summer patterns and test possible physical mechanisms behind them. This would have important implications for the predictability of extreme climate variability over Europe, especially at long timescales.

ACKNOWLEDGEMENTS

We thank two anonymous reviewers for their critical comments and valuable suggestions that lead to a significant improvement of our manuscript. This study is a contribution to the Helmholtz Association (HGF) climate initiative REKLIM Topic 8 'Rapid climate change derived from proxy data'. Funding by the AWI Strategy Fund Project – PalEX is gratefully acknowledged. We thank all researchers who make the data sets used in this study available.

ORCID

N. Rimbu https://orcid.org/0000-0003-2832-9396

REFERENCES

Barton, Y., Giannakaki, P., von Waldow, H., Chevalier, C., Pfahl, S. and Martius, O. (2016) Clustering of regional-scale extreme precipitation events in southern Switzerland. *Monthly Weather Review*, 144, 347–369. https://doi.org/10.1175/MWR-D-15-0205.1.

Bayerisches Landesamt für Umwelt. (2007) *Daily River Ammer Runoff Data from 1926 to 2006*. Germany: Munich.

Browning, K.A. (1997) The dry intrusion perspective of extra-tropical cyclone development. *Meteorolgy Applied*, 4, 317–324.

Camenisch, C., Keller, K.M., Salvisberg, M., Amann, B., Bauch, M., Blumer, S., Brázdil, R., Brönnimann, S., Büntgen, U., Campbell, B.M.S., Fernández-Donado, L., Fleitmann, D., Glaser, R., González-Rouco, F., Grosjean, M., Hoffmann, R.C., Huhtamaa, H., Joos, F., Kiss, A., Kotyza, O., Lehner, F., Luterbacher, J., Maughan, N., Neukom, R., Novy, T., Pribyl, K., Raible, C.C., Riemann, D., Schuh, M., Slavin, P., Werner, J.P. and Wetter, O. (2016) The 1430s: a cold period of extraordinary internal climate variability during the early Spörer minimum with social and economic impacts in north-western and central Europe. *Climate of the Past*, 12, 2107–2126. https://doi.org/10.5194/cp-12-2107-2016.

Cornes, R., van der Schrier, G., van den Besselaar, E.J.M. and Jones, P.D. (2018) An ensemble version of the E-OBS temperature and precipitation datasets. *Journal of Geophysical Research Atmophere*, 123, 9391–9409. https://doi.org/10.1029/2017JD028200.

Czymzik, M., Brauer, A., Dulski, P., Plessen, B., von Grafenstein, U., Naumann, R. and Scheffler, R. (2013) Orbital and solar forcing of shifts in mid- to late Holocene flood intensity from varved sediments of pre-alpine Lake Ammersee (southern Germany). *Quaternary Science Review*, 61, 96–110. https://doi.org/10.1016/j.quascirev.2012.11.010.

Czymzik, M., Dulski, P., Plessen, B., von Grafenstein, U., Naumann, R. and Brauer, A. (2010) A 450 year record of spring-summer flood layers in annually laminated sediments from Lake Ammersee (southern Germany). *Water Resources Research*, 46, W11528. https://doi.org/10.1029/2009WR008360.

Czymzik, M., Muscheler, R. and Brauer, A. (2016) Solar modulation of flood frequency in central Europe during spring and summer on inter-annual to multi-centennial time scales. *Climate of the Past*, 12, 799–805. https://doi.org/10.5194/cp-12-799-2016.

Davini, P., Cagnazzo, C., Gualdi, S. and Navarra, A. (2012) Bidimensional diagnostics, variability and trends of Northern Hemisphere blocking. *Journal of Climate*, 25, 6496–6509. https://doi.org/10.1175/JCLI-D-12-00032.1.

Dima, M. and Lohmann, G. (2009) Conceptual model for millennial climate variability: a possible combined solar-thermohaline circulation origin for the ~1500-year cycle. *Climate Dynamics*, 32, 301–311. https://doi.org/10.1007/s00382-008-0471-x.

Drouard, M. and Woolings, T. (2018) Contrasting mechanisms of summer blocking over western Eurasia. *Geophysical Research Letters*, 45, 12040–12048. https://doi.org/10.1029/2018GL079894.

Ghil, M., Allen, M.R., Dettinger, M.D., Ide, K., Kondrashov, D., Robertson, A.W., Saunders, A., Tian, Y., Vardi, F. and Yiou, P. (2002) Advanced spectral methods for climatic time-series. *Reviews of Geophysics*, 40, 1–41. https://doi.org/10.1029/2001RG000092.

Haigh, J.D. (1999) A GCM study of climate change in response to the 11-year solar cycle. *Quarterly Journal of Meteorological Society*, 125, 871–892.

Huth, R., Kysely, J., Bochnıcek, J. and Hejda, P. (2008) Solar activity affects the occurrence of synoptic types over Europe. *Annale Geophysics*, 26, 1999–2004.

Ineson, S., Scaife, A.A., Knight, J.R., Manners, J.C., Dunstone, N.J., Gray, L.J. and Haigh, J.D. (2011) Solar forcing of winter climate variability in the Northern Hemisphere. *Nature Geoscience*, 4, 753–757.

Ionita, M., Dima, M., Lohmann, G., Scholz, P. and Rimbu, N. (2015) Predicting the June 2013 European flooding based on precipitation, soil moisture and sea level pressure. *Journal of Hydrometeorology*, 16, 598–614. https://doi.org/10.1175/JHM-D-14-0156.1.

Kalnay, E., Kanamitsu, M., Kistler, R., Collins, W., Deaven, D., Gandin, L., Iredell, M., Saha, S., White, G., Woolen, J., Zhu, Y., Chelliah, M., Ebisuzaki, W., Higgins, W., Janowiak, J., Mo, K. C., Ropelewski, C., Wang, J., Leetmaa, A., Reynolds, R., Jenne, R. and Dennis, J. (1996) The NCEP/NCAR 40-year reanalysis project. *Bulletin American Meteorological Socciety*, 77, 437–470. https://doi.org/10.1175/1520-0477(1996)077<0437:TNYRP>2.0.CO;2.

Kaniewski, D., Marriner, N., Morhange, C., Faivre, S., Otto, T. and Van Campo, E. (2016) Solar pacing of storm surges, coastal flooding and agricultural losses in the Central Mediterranean. *Scientific Reports*, 6, 25197. https://doi.org/10.1038/srep25197.

Kornhuber, K., Petoukhov, V., Petri, S., Rahmstorf, S. and Coumou, D. (2016) Evidence for wave resonance as a key mechanism for generating high-amplitude quasi-stationary waves in boreal summer. *Climate Dynamics*, 49, 1961–1979. https://doi.org/10.1007/s00382-016-3399-6.

Krichak, S.O., Breitgand, J.S., Gualdi, S. and Feldstein, S. (2014) Teleconnection–extreme precipitation relationships over the Mediterranean region. *Theoretical and Applied Climatology*, 117, 679–692. https://doi.org/10.1007/s00704-013-1036-4.

Lockwood, M.A., Rouillard, P. and Finch, D. (2009) The rise and fall of open solar flux during the current grand solar maximum. *Astrophysics Journal*, 700, 937–944.

Lohmann, G., Rimbu, N. and Dima, M. (2004) Climate signature of solar irradiance variations: analysis of long-term instrumental, historical, and proxy data. *International Journal of Climatology*, 24, 1045–1056. https://doi.org/10.1002/joc.1054.

Lu, H., Franzke, C., Martius, O., Jarvis, M.J. and Phillips, T. (2013) Solar wind dynamic pressure effect on planetary wave propagation and synoptic-scale Rossby wave breaking. *Journal of Geophysical Research: Atmosphere*, 118, 4476–4493. https://doi.org/10.1002/jgrd.50374.

Ludwig, R., Tascher, S. and Mauser, W. (2013) Modelling floods in the Ammer catchment: limitations and challenges with a coupled meteo-hydrological model approach. *Hydrological Earth System Sciences*, 7, 833–847.

Martin-Puertas, C., Matthes, K., Brauer, A., Muscheler, R., Hansen, F., Petrick, C., Aldahan, A., Possnert, G. and van Geel, B. (2012) Regional atmospheric circulation shifts induced by a grad solar minimum. *Naure Geosciences*, 5, 397–401. https://doi.org/10.1038/NGEO1460.

Masato, G., Hoskins, B.J. and Woollings, T. (2013) Wave-breaking characteristics of Northern Hemisphere winter blocking: a two-dimensional approach. *Journal of Climate*, 26, 4535–4549. https://doi.org/10.1175/JCLI-D-12-00240.1.

Ogi, M., Tachibana, Y. and Yamazaki, K. (2003) Impact of the wintertime North Atlantic Oscillation (NAO) on the summer-time atmospheric circulation. *Geophysical Research Letters*, 30, 1704. https://doi.org/10.1029/2003GL017280.

Petoukhov, V., Rahmstorf, S., Petri, S. and Schellnhuber, H.J. (2013) Quasiresonant amplification of planetary waves and recent Northern Hemisphere weather extremes. *Proceedings of the National Academy of Sciences of the United States of America*, 110, 5336–5341. https://doi.org/10.1073/pnas.1222000110.

Petrow, T. and Merz, B. (2009) Trends in flood magnitude frequency and seasonality in Germany in the period 1951–2002. *Journal of Hydrology*, 371, 129–141. https://doi.org/10.1016/j.hydrol.2009.03.024.

Pfahl, S., Schwierz, C., Croci-Maspoli, M., Grams, C.M. and Wernli, H. (2015) Importance of latent heat release in ascending air streams for atmospheric blocking. *Nature Geoscience*, 8, 610–614. https://doi.org/10.1038/ngeo2487.

Rimbu, N., Czymzik, M., Ionita, M., Lohmann, G. and Brauer, A. (2016) Atmospheric circulation patterns associated with the variability of River Ammer floods: evidence from observed and proxy data. *Climate of the Past*, 12, 377–385. https://doi.org/10.5194/cp-12-377-2016.

Rimbu, N., Lohmann, G., Lorenz, S.J., Kim, J.H. and Schneider, R. R. (2004) Holocene climate variability as derived from alkenone sea surface temperature and coupled ocean-atmosphere model experiments. *Climate Dynamics*, 23, 215–227. https://doi.org/10.1007/s00382-004-0435-8.

Scafetta, N., Milani, F., Bianchi, A. and Ortolani, V. (2016) On the astronomical origin of the Hallstatt oscillation found in radiocarbon and climate records throughout the Holocene. *Earth Science Review*, 162, 24–43. https://doi.org/10.1016/j.earscirev.2016.09.004.

Scherer, S., Croci-Maspoli, M., Schwierz, C. and Appenzeller, C. (2006) Two-dimensional indices of atmospheric blocking and their statistical relationship with winter climate patterns in the Euro-Atlantic region. *International Journal of Climatology*, 26, 233–249. https://doi.org/10.1002/joc.1250.

Schlemmer, L., Martius, O., Sprenger, M., Schwierz, C. and Twitchett, A. (2010) Disentangling the forcing mechanisms of heavy precipitation event along the Alpine south side using potential vorticity inversion. *Monthly Weather Review*, 138, 2336–2353. https://doi.org/10.1175/2009MWR3202.1.

Simpson, I., Blackburn, M. and Haigh, J. (2009) The role of eddies in driving the tropospheric response to stratospheric heating perturbations. *Journal of Atmospheric Sciences*, 66, 1347–1365. https://doi.org/10.1175/2008JAS2758.1.

Slivinski, L.C., Compo, G.P., Whitaker, J.S., Sardeshmukh, P.D., Giese, B.S., McColl, C., Allan, R., Yin, X., Vose, R., Titchner, H., Kennedy, J., Spencer, L.J., Ashcroft, L., Brönnimann, S., Brunet, M., Camuffo, D., Cornes, R., Cram, T. A., Crouthamel, R., Domínguez-Castro, F., Freeman, J.E., Gergis, J., Hawkins, E., Jones, P.D., Jourdain, S., Kaplan, A., Kubota, H., Le Blancq, F., Lee, T.-.C., Lorrey, A., Luterbacher, J., Maugeri, M., Mock, C.J., Moore, G.W.K., Przybylak, R., Pudmenzky, C., Reason, C., Slonosky, V.C., Smith, C.A., Tinz, B., Trewin, B., Valente, M.A., Wang, X.L., Wilkinson, C., Wood, K. and Wyszyński, P. (2019) Towards a more reliable historical reanalysis: improvements for version 3 of the twentieth century reanalysis system. *Quarterly Journal of Royal Meteorological Society*, 145(724), 2876–2908. https://doi.org/10.1002/qj.3598.

Solanki, S.K., Usoskin, I.G., Kromer, B., Schussler, M. and Beer, J. (2004) Unusual activity of the sun during recent decades compared to the previous 11,000 years. *Nature*, 431, 1084–1087. https://doi.org/10.1038/nature02995.

Steinhilber F., Beer J., Fröhlich, C. (2009) Total solar irradiance during the Holocene. *Geophysical Research Letters*, 36 (19), L19704. http://dx.doi.org/10.1029/2009gl040142.

Swierczynski, T., Brauer, A., Lauterbach, S., Marin-Puertas, C., Dulsky, P., von Grafenstein, U. and Rohr, C. (2012) A 1600 yr seasonally resolved record of decadal-scale flood variability from the Austrian Pre-Alps. *Geology*, 40, 1047–1050. https://doi.org/10.1130/G33493.1.

Tibaldi, S. and Molteni, F. (1990) On the operational predictability of blocking. *Tellus A*, 42, 343–365. https://doi.org/10.1034/j.1600-0870.1990.t01-2-00003.x.

Wick, L. and Tinner, W. (1997) Vegetation changes and timberline fluctuations in the Central Alps as indicators of Holocene climatic oscillations. *Arctic and Alpine Research*, 29(4), 445–458. https://doi.org/10.2307/1551992.

Wilhelm, B., Canovas, J.A.B., Macdonald, N., Toonen, W.H.J., Baker, V., Barriendos, M., Benito, G., Brauer, A., Corella, J.P., Denniston, R., Glaser, R., Ionita, M., Kahle, M., Liu, T., Lutscher, M., Macklin, M., Mudelsee, M., Munoz, S., Schulte, L., George, S., Stoffel, M. and Wetter, O. (2018) Interpreting historical, botanical, and geological evidence to aid preparations for future floods. *WIREs Water*, 6, 1–22. https://doi.org/10.1002/wat2.1318.

Wirth, S.B., Glur, L., Gilli, A. and Anselmetti, F.S. (2013) Holocene flood frequency across the Central Alps – solar forcing and evidence for variations in North Atlantic atmospheric circulation. *Quaternary Science Review*, 80, 112–128.

Woolings, T., Barriopedro, D., Methven, J., Son, S.-W., Martius, O., Harvey, B., Silmann, J., Lupo, A. and Seneviratne, S. (2018) Blocking and its response to climate change. *Current Climate Change Reports*, 4, 287–300. https://doi.org/10.1007/s40641-018-0108-z.

Woolings, T., Lockwood, M., Masato, G., Bell, C. and Gray, L. (2010) Enhanced signature of solar variability in Eurasian winter climate. *Geophysical Research Letters*, 37, L20805. https://doi.org/10.1029/2010GL044601.

Zhang, X., Alexander, L., Hegerl, G., Jones, P.D. and Klein Tank, A. (2011) Indices for monitoring changes in extremes based on daily temperature and precipitation data. *WIREs Climate Change*, 2, 851–870. https://doi.org/10.1002/wcc.147.

SUPPORTING INFORMATION

Additional supporting information may be found online in the Supporting Information section at the end of this article.

How to cite this article: Rimbu N, Lohmann G, Ionita M, Czymzik M, Brauer A. Interannual to millennial-scale variability of River Ammer floods and its relationship with solar forcing. *Int J Climatol*. 2021;41 (Suppl. 1):E644–E655. https://doi.org/10.1002/joc.6715